BULLETIN OF THE CHEMICAL SOCIETY OF JAPAN VOL. 41, 1798—1808 (1968)

Intrachain Force Field and Normal Vibrations of Polyethylene Glycol

Hiroatsu MATSUURA and Tatsuo MIYAZAWA
Institute for Protein Research, Osaka University, Kita-ku, Osaka

(Received January 29, 1968)

Normal vibrations of polyethylene glycol and the perdeuterated species were treated. Intrachain force field was expressed in terms of local-symmetry coordinates. Force constants were adjusted by the method of least squares, with reference to observed infrared and Raman frequencies. A set of force constants was obtained, which reproduces the observed frequencies with an r.m.s. deviation of 0.9%. The values of the force constants thus refined were discussed in comparison with corresponding values of related molecules. Vibrational assignments of the observed infrared absorption bands and Raman lines were revised on the basis of potential-energy distributions refined in the present treatment.

The chain vibrations of an isolated helical molecule are specified with the phase difference δ between the vibrational displacements of the corresponding atoms in neighboring repeat units. The selection rules for the infrared absorption and Raman scattering are related with the angle θ of rotation, per unit, about the helix axis. Thus, the infrared bands arise from the chain vibrations with $\delta=0$ or θ and the Raman lines arise from the vibrations with $\delta=0$, θ, or 2θ.[1,2] For the neutron scattering, there is no selection rule

1) P. Higgs, *Proc. Roy. Soc.* (*London*), **A 220**, 472 (1953).
2) T. Miyazawa, *J. Chem. Phys.*, **35**, 693 (1961); *Nippon Kagaku Zasshi* (*J. Chem. Soc. Japan, Pure Chem. Sect.*), **88**, 111 (1967); H. Sugeta and T. Miyazawa, *J. Chem. Phys.*, **47**, 2034 (1967).

and accordingly the frequency-distribution peaks give rise to inelastic scattering peaks.

The X-ray diffraction and infrared and Raman spectra of polyethylene glycol have been studied, and this polymer chain has been found to contain seven chemical units of CH_2CH_2O and two helical turns per fiber period.[3-6] The internal-rotation conformation about the O-CH_2, CH_2-CH_2, and CH_2-O bonds are trans, gauche, and trans, respectively. The vibrational frequencies calculated for the 7_2 helix conformation agree satisfactorily well with the observed frequencies of the far-infrared bands below 300 cm^{-1}.

For the polyethylene-glycol chain, the repeat unit contains seven atoms, and accordingly, there are twenty-one branches of the chain vibrations. In the region below 600 cm^{-1}, there are six branches associated with C-C-O and C-O-C angle-bending modes and internal-rotation modes about C-C and C-O bonds. From dispersion curves (frequency *versus* phase difference) for these branches, frequency distribution of the chain vibrations has been calculated,[7] in comparison with neutron inelastic scattering peaks.[8] Also, Young's modulus along the chain axis may be treated by the use of the intrachain force field. For the polyethylene-glycol chain, the calculated value[7] of 0.008 mdyn/Å^2 agrees closely with the experimental value[9] of 0.010 mydn/Å^2.

Thus, the infrared and Raman frequencies, frequency distribution and neutron inelastic scattering, and Young's modulus may be treated systematically on the basis of the intrachain force field. An extensive study on the force field of the polyethylene-glycol chain is also important for analyses of infrared and Raman spectra of model molecules[10] $RO(-CH_2CH_2O-)_pR$ [R: H, D or CH_3; p= 1−7] and of molten polyethylene glycol.[11]

In the present study, the intrachain force field of polyethylene glycol was refined, by the method of least squares, with reference to the observed infrared and Raman frequencies.[4,5] Nature of the infrared and/or Raman active vibrations was elucidated, referring to the calculated potential-energy distributions.

Normal Coordinate Treatment

For the 7_2 helix conformation of polyethylene glycol, the unit rotation about the axis is given as $\theta=4\pi/7$. Also, as confirmed by the analysis of the parallel infrared bands, the molecular chain has two twofold axes per repeat unit; one axis bisects the C-O-C bond-angle while the other axis intersects the C-C bond at right angle. Accordingly, the non-degenerate A vibrations (with $\delta=0$) are classified into the A_1 and A_2 vibrations which are symmetric and antisymmetric, respectively, with respect to the twofold axes.[12] The parallel infrared bands of polyethylene glycol are due to the A_2 vibrations with $\delta=0$ while the perpendicular bands are due to the E_1 vibrations with $\delta=4\pi/7$. The Raman lines are due to the A_1, E_1, or E_2 vibrations with $\delta=8\pi/7$.

In the present study, the A_1, A_2, and E_1 vibrations were treated for the normal species $(-CH_2CH_2O-)_p$ and the perdeuterated species $(-CD_2CD_2O-)_p$ of the polyethylene-glycol chain. The general method for treating the helical chain vibrations[2] was used. The stretching (Δr), angle-bending ($\Delta\phi$), and internal-rotation coordinates (Δt)[13] were denoted with the atom indices given previously[4] (see also Fig. 1). The internal coordinates

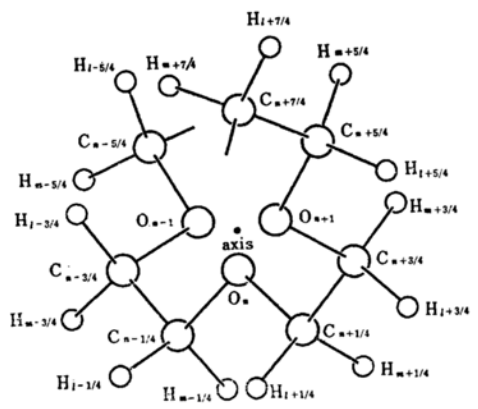

Fig. 1. Numbering of atoms of polyethylene glycol as used in the normal coordinate treatment.

3) T. Miyazawa, *J. Polymer Sci.*, **55**, 215 (1961), addendum.
4) T. Miyazawa, K. Fukushima and Y. Ideguchi, *J. Chem. Phys.*, **37**, 2764 (1962).
5) H. Tadokoro, Y. Chatani, T. Yoshihara, S. Tahara and S. Murahashi, *Makromol. Chem.*, **73**, 109 (1964).
6) T. Yoshihara, H. Tadokoro and S. Murahashi, *J. Chem. Phys.*, **41**, 2902 (1964).
7) H. Matsuura and T. Miyazawa, *Rept. Progr. Polymer Phys. Japan*, **9**, 179 (1966).
8) S. Trevino and H. Boutin, *J. Macromol. Sci.*, **A1**, 723 (1967).
9) I. Sakurada, T. Ito and K. Nakamae, *J. Polymer Sci.*, **C15**, 75 (1966).
10) H. Matsuura and T. Miyazawa, Symposium on Molecular Structure, Toyonaka, 1966; *Rept. Progr. Polymer Phys. Japan*, **10**, 187 (1967).
11) H. Matsuura and T. Miyazawa, Annual Meeting of the Chemical Society of Japan, Tokyo, 1967.
12) C. Y. Liang and S. Krimm, *J. Chem. Phys.*, **25**, 563 (1956).
13) T. Miyazawa and K. Fukushima, *J. Mol. Spectry.*, **15**, 308 (1965).

were then transformed into the local-symmetry coordinates ($\sigma's$),[14] namely σ_{ss} (CH_2 symmetric stretching), σ_{as} (CH_2 antisymmetric stretching), σ_{sc} (CH_2 scissoring), σ_{wa} (CH_2 wagging), σ_{tw} (CH_2 twisting), σ_{ro} (CH_2 rocking), σ_{CCst} (C-C stretching), σ_{COst} (C-Ostretching), σ_{CCO} (C-C-O bending), σ_{COC} (C-O-C bending), σ_{CCto} (C-C internal-rotation), and σ_{COto} (C-O internal-rotation). These coordinates were grouped into four vectors,

$$\boldsymbol{R}^s_n,\ \boldsymbol{R}_{n+1/4},\ \boldsymbol{R}^s_{n+1/2},\ \text{and}\ \boldsymbol{R}_{n+3/4}.$$

$$\begin{aligned}
\boldsymbol{R}^s_n:\quad & \sigma_{COC}=\Delta\phi(C_{n-1/4}\text{-}O_n\text{-}C_{n+1/4})\\
\boldsymbol{R}_{n+1/4}:\quad & \sigma_{ss}=[\Delta r(C_{n+1/4}\text{-}H_{m+1/4})+\Delta r(C_{n+1/4}\text{-}H_{l+1/4})]/2^{1/2}\\
& \sigma_{as}=[\Delta r(C_{n+1/4}\text{-}H_{m+1/4})-\Delta r(C_{n+1/4}\text{-}H_{l+1/4})]/2^{1/2}\\
& \sigma_{sc}=[4\Delta\phi(H_{m+1/4}\text{-}C_{n+1/4}\text{-}H_{l+1/4})-\Delta\phi(H_{m+1/4}\text{-}C_{n+1/4}\text{-}C_{n+3/4})\\
& \qquad -\Delta\phi(H_{m+1/4}\text{-}C_{n+1/4}\text{-}O_n)-\Delta\phi(H_{l+1/4}\text{-}C_{n+1/4}\text{-}C_{n+3/4})\\
& \qquad -\Delta\phi(H_{l+1/4}\text{-}C_{n+1/4}\text{-}O_n)]/20^{1/2}\\
& \sigma_{wa}=[\Delta\phi(H_{m+1/4}\text{-}C_{n+1/4}\text{-}C_{n+3/4})-\Delta\phi(H_{m+1/4}\text{-}C_{n+1/4}\text{-}O_n)\\
& \qquad +\Delta\phi(H_{l+1/4}\text{-}C_{n+1/4}\text{-}C_{n+3/4})-\Delta\phi(H_{l+1/4}\text{-}C_{n+1/4}\text{-}O_n)]/2\\
& \sigma_{tw}=[\Delta\phi(H_{m+1/4}\text{-}C_{n+1/4}\text{-}C_{n+3/4})-\Delta\phi(H_{m+1/4}\text{-}C_{n+1/4}\text{-}O_n)\\
& \qquad -\Delta\phi(H_{l+1/4}\text{-}C_{n+1/4}\text{-}C_{n+3/4})+\Delta\phi(H_{l+1/4}\text{-}C_{n+1/4}\text{-}O_n)]/2\\
& \sigma_{ro}=[\Delta\phi(H_{m+1/4}\text{-}C_{n+1/4}\text{-}C_{n+3/4})+\Delta\phi(H_{m+1/4}\text{-}C_{n+1/4}\text{-}O_n)\\
& \qquad -\Delta\phi(H_{l+1/4}\text{-}C_{n+1/4}\text{-}C_{n+3/4})-\Delta\phi(H_{l+1/4}\text{-}C_{n+1/4}\text{-}O_n)]/2\\
& \sigma_{COst}=\Delta r(C_{n+1/4}\text{-}O_n)\\
& \sigma_{CCO}=[5\Delta\phi(C_{n+3/4}\text{-}C_{n+1/4}\text{-}O_n)-\Delta\phi(H_{m+1/4}\text{-}C_{n+1/4}\text{-}H_{l+1/4})\\
& \qquad -\Delta\phi(H_{m+1/4}\text{-}C_{n+1/4}\text{-}C_{n+3/4})-\Delta\phi(H_{m+1/4}\text{-}C_{n+1/4}\text{-}O_n)\\
& \qquad -\Delta\phi(H_{l+1/4}\text{-}C_{n+1/4}\text{-}C_{n+3/4})-\Delta\phi(H_{l+1/4}\text{-}C_{n+1/4}\text{-}O_n)]/30^{1/2}\\
& \sigma_{COto}=\Delta t(C_{n+1/4}\text{-}O_n)\\
\boldsymbol{R}^s_{n+1/2}:\quad & \sigma_{CCst}=\Delta r(C_{n+1/4}\text{-}C_{n+3/4})\\
& \sigma_{CCto}=\Delta t(C_{n+1/4}\text{-}C_{n+3/4})
\end{aligned}\qquad (1)$$

The elements of the $\boldsymbol{R}_{n+3/4}$ vector may be derived from the $\boldsymbol{R}_{n+1/4}$ vector by interchanging the subscripts, $n \leftrightarrow n+1$, $n+1/4 \leftrightarrow n+3/4$, $l+1/4 \leftrightarrow m+3/4$, and $m+1/4 \leftrightarrow l+3/4$.

The inverse kinetic-energy matrix $\boldsymbol{G}$ or the potential-energy matrix $\boldsymbol{F}$ for the infinite helical chain may be factored into the matrices associated with the symmetry coordinate vectors for the phase difference δ. The symmetry coordinates for polyethylene glycol were constructed as follow,

$$\begin{aligned}
\boldsymbol{S}_1(\delta)&=(2/N)^{1/2}\sum_n \boldsymbol{R}^s_n\cos n\delta\\
\boldsymbol{S}_3(\delta)&=(2/N)^{1/2}\sum_n \boldsymbol{R}^s_{n+1/2}\cos(n+1/2)\delta\\
\boldsymbol{S}_5(\delta)&=(1/N)^{1/2}\sum_n[\boldsymbol{R}_{n+1/4}\cos(n+1/4)\delta+\boldsymbol{R}_{n+3/4}\cos(n+3/4)\delta]\\
\boldsymbol{S}_6(\delta)&=(1/N)^{1/2}\sum_n[\boldsymbol{R}_{n+1/4}\cos(n+1/4)(\delta+2\pi)+\boldsymbol{R}_{n+3/4}\cos(n+3/4)(\delta+2\pi)]
\end{aligned}$$

and

$$\begin{aligned}
\boldsymbol{S}_1'(\delta)&=-(2/N)^{1/2}\sum_n \boldsymbol{R}^s_n\sin n\delta\\
\boldsymbol{S}_3'(\delta)&=-(2/N)^{1/2}\sum_n \boldsymbol{R}^s_{n+1/2}\sin(n+1/2)\delta\\
\boldsymbol{S}_5'(\delta)&=-(1/N)^{1/2}\sum_n[\boldsymbol{R}_{n+1/4}\sin(n+1/4)\delta+\boldsymbol{R}_{n+3/4}\sin(n+3/4)\delta]\\
\boldsymbol{S}_6'(\delta)&=-(1/N)^{1/2}\sum_n[\boldsymbol{R}_{n+1/4}\sin(n+1/4)(\delta+2\pi)+\boldsymbol{R}_{n+3/4}\sin(n+3/4)(\delta+2\pi)]
\end{aligned}\qquad (2)$$

where $(2/N)^{1/2}$ or $(1/N)^{1/2}$ is the normalization factor. The symmetry coordinate $S(\delta)$ is symmetric with respect to the twofold axis passing through the zeroth oxygen atom, whereas $S'(\delta)$ is antisymmetric with respect to this axis. Accordingly, the inverse kinetic-energy matrix (or potential-energy matrix) for the phase difference δ is factored into the $\boldsymbol{G}(\delta)$ [or $\boldsymbol{F}(\delta)$] associated with $S(\delta)$'s and the other identical one associated with $S'(\delta)$'s.

For calculating $\boldsymbol{G}(\delta)$ matrices, the bond lengths of r(C-C)=1.54 A, r(C-O)=1.43 A, and r(C-H)=1.09 Å, and tetrahedral bond angles were used. From these bond lengths and angles and the fiber period[15] of 19.25 Å,

14) T. Shimanouchi, *Nippon Kagaku Zasshi* (*J. Chem. Soc. Japan, Pure Chem. Sect.*), **86**, 261, 768 (1965); Symposium on Molecular Structure, Tokyo, 1964; Toyonaka, 1966.

15) E. R. Walter and F. P. Reding, National Meeting of the American Chemical Society, San Francisco, 1958.

the internal-rotation angles about the C–C and C–O bonds were calculated as 63°55′ and 188°51′, respectively, by the use of equations for helical parameters.[3,16] The atomic masses of 12.01115 for carbon, 15.99940 for oxygen, 1.00797 for hydrogen, and 2.01410 for deuterium were used for calculating the $\boldsymbol{G}(\delta)$ matrix elements.

For degenerate vibrations, phase angles $\varepsilon(\delta)$ are useful for describing phase relations in normal modes. Setting $\varepsilon=0$ for internal coordinates $\boldsymbol{R}^s_n(\delta)$, the phase angle for $\boldsymbol{R}^s_{n+1/2}(\delta)$ is given as $\varepsilon=\delta/2$. The phase angles for $[\boldsymbol{R}_{n+1/4}(\delta)]_k$*1 and $[\boldsymbol{R}_{n+3/4}(\delta)]_k$ are given as $\varepsilon_k=\delta/2-\varepsilon'_k(\delta)$ and $\varepsilon_k=\delta/2+\varepsilon'_k(\delta)$, respectively, where the values of $\varepsilon'_k(\delta)$ may be calculated from the eigenvector components for the kth coordinates.[2] Then, the phase-angle difference between $[\boldsymbol{R}_{n+1/4}(\delta)]_k$ and $[\boldsymbol{R}_{n+3/4}(\delta)]_k$ is $\Delta\varepsilon_k(\mathrm{OCH_2\text{-}CH_2O})=2\varepsilon'_k(\delta)$. Vibrational modes with $\Delta\varepsilon_k(\mathrm{OCH_2\text{-}CH_2O})\sim0$ and $\sim\pm180°$ are quasi-symmetric and quasi-antisymmetric, respectively, with respect to the twofold axis that intersects the CH_2–CH_2 bond. The phase-angle difference between $[\boldsymbol{R}_{n-1/4}(\delta)]_k$ and $[\boldsymbol{R}_{n+1/4}(\delta)]_k$ is $\Delta\varepsilon_k(\mathrm{C\text{-}O\text{-}C})=\delta-2\varepsilon'_k(\delta)$. Vibrational modes with $\Delta\varepsilon_k(\mathrm{C\text{-}O\text{-}C})\sim0$ and $\sim\pm180°$ are quasi-symmetric and quasi-antisymmetric, respectively, with respect to the twofold axis that intersects the C–O–C angle. It may be remarked that the phase-angle differences for the A_1 and A_2 vibrations are $\Delta\varepsilon=0$ and 180°, respectively.

Numerical calculations in the present treatment of normal vibrations were carried out with a HITAC 5020 E computer (Hitachi, Limited) at the University of Tokyo and a NEAC 2200-500 computer (Nippon Electric Company, Limited) at Osaka University.

Potential Function

In a previous study,[4] the Urey-Bradley force field (UBFF)[17] with supplementary terms was used, and the potential constants were transferred from polyethylene, dimethyl ether, and propyl alcohol. In the present treatment, however, a more generalized potential function (local-symmetry force field)[14] was used. Accordingly, the infinite potential-energy matrix of the infinite polyethylene-glycol chain is expressed in terms of the local-symmetry coordinate vectors. Nonzero submatrices in the lower half columns associated with $\boldsymbol{R}^s_n$, $\boldsymbol{R}_{n+1/4}$, $\boldsymbol{R}^s_{n+1/2}$, and $\boldsymbol{R}_{n+3/4}$ are shown below:

	$\tilde{\boldsymbol{R}}^s_n$	$\tilde{\boldsymbol{R}}_{n+1/4}$	$\tilde{\boldsymbol{R}}^s_{n+1/2}$	$\tilde{\boldsymbol{R}}_{n+3/4}$
$\boldsymbol{R}^s_n$	$\boldsymbol{A}^a_0$			
$\boldsymbol{R}_{n+1/4}$	$\tilde{\boldsymbol{F}}^a_{1/4}\boldsymbol{C}_0$			
$\boldsymbol{R}^s_{n+1/2}$	0	$\boldsymbol{F}^b_{1/4}$	$\boldsymbol{A}^b_0$	
$\boldsymbol{R}_{n+3/4}$	0	$\boldsymbol{C}^b_{1/2}$	$\tilde{\boldsymbol{F}}^b_{1/4}$	$\boldsymbol{C}_0$
$\boldsymbol{R}^s_{n+1}$	0	0	0	$\boldsymbol{F}^a_{1/4}$
$\boldsymbol{R}_{n+5/4}$	0	0	0	$\boldsymbol{C}^a_{1/2}$
$\boldsymbol{R}^s_{n+3/2}$	0	0	0	0

where the matrices with tilde are the transposed matrices. The elements of the submatrices are given below:

$$\boldsymbol{A}^a_0=[f(\mathrm{COC})]$$

$$\boldsymbol{A}^b_0=\begin{bmatrix} f(\mathrm{CC\ st}) & 0 \\ 0 & f(\mathrm{CC\ to}) \end{bmatrix}$$

$$\boldsymbol{C}_0=\begin{bmatrix}
f(\mathrm{ss}) & & & & & & & & \\
0 & f(\mathrm{as}) & & & & & & & \\
* & 0 & f(\mathrm{sc}) & & & & & & \\
* & 0 & f\begin{pmatrix}\mathrm{sc}\\ \mathrm{wa}\end{pmatrix} & f(\mathrm{wa}) & & & & & \\
0 & * & 0 & 0 & f(\mathrm{tw}) & & & & \\
0 & * & 0 & 0 & f\begin{pmatrix}\mathrm{tw}\\ \mathrm{ro}\end{pmatrix} & f(\mathrm{ro}) & & & \\
* & 0 & * & * & 0 & 0 & f(\mathrm{CO\ st}) & & \\
* & 0 & f\begin{pmatrix}\mathrm{sc}\\ \mathrm{CCO}\end{pmatrix} & f\begin{pmatrix}\mathrm{wa}\\ \mathrm{CCO}\end{pmatrix} & 0 & 0 & f\begin{pmatrix}\mathrm{CO\ st}\\ \mathrm{CCO}\end{pmatrix} & f(\mathrm{CCO}) & \\
0 & 0 & 0 & 0 & 0 & 0 & 0 & 0 & f(\mathrm{CO\ to})
\end{bmatrix}$$

(symmetric)

16) H. Sugeta and T. Miyazawa, *Biopolymers*, **5**, 673 (1967).

*1 The subscript k indicates the kth component of internal-coordinate vectors.

17) T. Shimanouchi, *J. Chem. Phys.*, **17**, 245, 734, 848 (1949); *Pure Appl. Chem.*, **7**, 131 (1963).

$$C^a_{1/2}=\begin{bmatrix} 0 & & & & & & & & & \\ 0 & 0 & & & & & & & & \\ 0 & 0 & 0 & & & \text{symmetric} & & & & \\ 0 & 0 & 0 & 0 & & & & & & \\ 0 & 0 & 0 & 0 & 0 & & & & & \\ 0 & 0 & 0 & 0 & 0 & 0 & & & & \\ 0 & 0 & 0 & 0 & 0 & 0 & f\binom{\text{CO st}}{\text{CO st}} & & & \\ 0 & 0 & 0 & 0 & 0 & 0 & 0 & 0 & & \\ 0 & 0 & 0 & 0 & 0 & 0 & 0 & 0 & 0 & \end{bmatrix}$$

$$C^b_{1/2}=\begin{bmatrix} 0 & & & & & & & & & \\ 0 & 0 & & & & & & & & \\ 0 & 0 & 0 & & & \text{symmetric} & & & & \\ 0 & 0 & 0 & f'\binom{\text{wa}}{\text{wa}} & & & & & & \\ 0 & 0 & 0 & 0 & f'\binom{\text{tw}}{\text{tw}} & & & & & \\ 0 & 0 & 0 & 0 & 0 & f'\binom{\text{ro}}{\text{ro}} & & & & \\ 0 & 0 & 0 & 0 & 0 & 0 & 0 & & & \\ 0 & 0 & 0 & 0 & 0 & f'\binom{\text{ro}}{\text{CCO}} & 0 & f'\binom{\text{CCO}}{\text{CCO}} & & \\ 0 & 0 & 0 & 0 & 0 & 0 & 0 & 0 & 0 & \end{bmatrix}$$

$$F^a_{1/4}=\begin{bmatrix} 0 & 0 & 0 & 0 & 0 & 0 & f\binom{\text{CO st}}{\text{COC}} & f'\binom{\text{CCO}}{\text{COC}} & 0 \end{bmatrix}$$

$$F^b_{1/4}=\begin{bmatrix} * & 0 & * & * & 0 & 0 & f\binom{\text{CC st}}{\text{CO st}} & f\binom{\text{CC st}}{\text{CCO}} & 0 \\ 0 & 0 & 0 & 0 & 0 & 0 & 0 & 0 & 0 \end{bmatrix}$$

where the elements denoted with asterisk are related with the UBFF's repulsion constants, F(HCO), F(HCC), and F(HCH).

The force constants f(ss), f(as), f(sc), f(wa), f(tw), f(ro), f(CC st), f(CO st), f(CCO), f(COC), f(CC to), and f(CO to) are diagonal elements associated with the local-symmetry coordinates shown in parentheses. The non-diagonal elements of UBFF, namely, f(sc, wa), f(sc, CCO), f(wa, CCO), f(tw, ro), f(CO st, CCO), f(CO st, CO st), f(CO st, COC), f(CC st, CO st), f(CC st, CCO), and F(HCO), F(HCC), and F(HCH) were taken as independent force constants. The potential constants denoted with primes f'(wa, wa), f'(tw, tw), f'(ro, ro), f'(CCO, CCO), f'(ro, CCO), and f'(COC, CCO) are not found in the simple UBFF. However, these constants were also taken into account as supplementary elements, which are associated with the vibrational interactions between the adjacent methylene groups or between the adjacent skeletal-bond angles.

In the beginning, the modified UBFF constants of the previous studies[4,7] were transformed into the constants of the local-symmetry force field (LSFF). The LSF Fforce constants were then adjusted by the method of least squares,[18] with reference to the infrared absorption frequencies of the normal and perdeuterated species of polyethylene glycol,[4,5] and the Raman frequencies of the normal species.[19,20] The observed frequencies[21] of p-dioxane and p-dioxane-d_8 were also used in the refinement, since these molecules consist of the same chemical units of CH_2CH_2O and CD_2CD_2O, respectively, as those of the normal and perdeuterated species of this polymer. The force constants thus obtained are shown in Table 1. The observed and calculated frequencies are listed in Table 2—5, together with the potential-energy distributions (P. E. D.)[22] defined as follows,

$$(P.E.D.)_{ia}=(F_{ii}L^2_{ia}/\lambda_a)\times 100 \qquad (3)$$

where F_{ii} is the ith diagonal element of the potential-energy matrix, L_{ia} is the ith element of the ath eigenvector, and λ_a is the

18) D. E. Mann, T. Shimanouchi, J. H. Meal and L. Fano, *J. Chem. Phys.*, **27**, 43 (1957).

19) Y. Matsui, T. Kubota, H. Tadokoro and T. Yoshihara, *J. Polymer Sci.*, **A3**, 2275 (1965).

20) R. F. Schaufele, *Trans. New York Acad. Sci.*, to be published.

21) H. Matsuura and T. Miyazawa, Symposium on Molecular Structure, Sapporo, 1967.

22) Y. Morino and K. Kuchitsu, *J. Chem. Phys.*, **20**, 1809 (1952); I. Nakagawa, *Nippon Kagaku Zasshi* (*J. Chem. Soc. Japan, Pure Chem. Sect.*), **74**, 243 (1953).

TABLE 1. INTRACHAIN POTENTIAL CONSTANTS OF POLYETHYLENE GLYCOL

f(ss)	4.711[a]	f(tw, ro)	−0.140[b]	f(CCO)	1.063[b]	f'(ro, ro)	0.026[b]
f(as)	4.694[a]	f(CC st, CO st)	0.395[a]	f(COC)	1.523[b]	f'(CCO, CCO)	−0.127[b]
f(sc)	0.577[b]	f(CO st, CO st)	0.340[a]	f(CC to)	0.113[b]	f'(ro, CCO)	0.178[b]
f(wa)	0.739[b]	f(CC st, CCO)	0.017[c]	f(CO to)	0.099[b]	f'(CCO, COC)	−0.029[b]
f(tw)	0.681[b]	f(CO st, CCO)	0.455[c]	f(sc, wa)	0.026[b]	F(HCO)	0.889[d]
f(ro)	0.778[b]	f(CO st, COC)	0.259[c]	f(sc, CCO)	0.028[b]	F(HCC)	0.317[d]
f(CC st)	4.208[a]	f'(wa, wa)	0.028[b]	f(wa, CCO)	−0.004[b]	F(HCH)	0.200[d]
f(CO st)	5.227[a]	f'(tw, tw)	0.017[b]				

a) In unit of mdyn·Å. b) In unit of mdyn·Å. c) In unit of mdyn.
d) Repulsion constants of Urey-Bradley force field in unit of mdyn/Å, F' is taken as $-F/10$.

TABLE 2. OBSERVED AND CALCULATED FREQUENCIES (cm^{-1}) AND POTENTIAL-ENERGY DISTRIBUTIONS FOR THE A_1 AND A_2 VIBRATIONS OF NORMAL POLYETHYLENE GLYCOL $(-CH_2CH_2O-)_p$

	Obs. freq.[a] Infrared[b]	Raman[c]	Calc. freq.	Potential-energy distributions
		2939 m	2940	CH_2 antisym stretch (101)
			2874	CH_2 sym stretch (101)
		1484 s	1479	CH_2 scissor (98)
		1398 w	1423	CH_2 wag (88), CC stretch (20)
		(1235)	1252	CH_2 twist (81)
A_1	inactive	1126 m	1137	CH_2 rock (36), CO stretch (18)
		(1064)	1073	CO stretch (47), CC stretch (46)
		861 m	866	CO stretch (50), CH_2 rock (46)
		279 w	274	CCO bend (24), CC internal-rotation (19), COC bend (17)
		216 w	218	COC bend (48), CO internal-rotation (22)
			2943	CH_2 antisym stretch (101)
	2890 s		2883	CH_2 sym stretch (100)
	1463, 1457 m		1470	CH_2 scissor (100)
	1345 s		1344	CH_2 wag (107)
A_2	1244 m	inactive	1264	CH_2 twist (81)
	1102 vs		1087	CO stretch (94)
	963 s		964	CH_2 rock (49), CH_2 twist (18)
	529, 508 w		533	CCO bend (89), CH_2 rock (33)
	107 w		105	CO internal-rotation (90)

a) Relative intensities are shown after the frequencies;
vs: very strong, s: strong, m: medium, w: weak, and sh: shoulder.
b) Ref. 4. c) Ref. 20.

ath eigenvalue (frequency parameter).

For E_1 vibrations listed in Tables 3 and 5, phase-angle differences $\Delta\varepsilon(OCH_2\text{–}CH_2O)$ are given for CH_2 (or CD_2) sym. and antisym. stretch., scissor., wag., twist., and rock. modes and CCO bend. mode, while $\Delta\varepsilon$(C–O–C) are given for CO stretch. and internal-rotation modes.

Potential Constants

The potential constants for the polyethylene-glycol chain are listed in Table 1. By the use of these constants, calculated frequencies agree closely with observed frequencies, with a root-mean-square deviation as small as 0.9%.

The potential constants of methylene groups of polyethylene glycol (Table 1) may be compared with those of hydrocarbons[14] and polyethylene.[23] For example, symmetric- [f(ss)] and antisymmetric-stretching [f(as)] and scissoring constants [f(sc)] are nearly the same for polyethylene glycol (4.71 and 4.69 mdyne/Å and 0.58 mdyn·Å) and for propane (4.74 and 4.66 mdyn·Å and 0.59 mdyn·Å). However, the wagging constant [f(wa)] of polyethylene glycol (0.74 mdyn·Å) is appreciably larger than those of propane (0.64 mdyn·Å), and polyethylene (0.67 mdyn·Å), possibly due

23) M. Tasumi, T. Shimanouchi and T. Miyazawa, *J. Mol. Spectry.*, **11**, 422 (1963).

TABLE 3. OBSERVED AND CALCULATED FREQUENCIES (cm^{-1}), POTENTIAL-ENERGY DISTRIBUTIONS AND PHASE-ANGLE DIFFERENCES FOR THE E_1 VIBRATIONS OF NORMAL POLYETHYLENE GLYCOL $(-CH_2CH_2O-)_p$

Obs. freq.[a] Infrared[b]	Raman[c]	Calc. freq.	Potential-energy distributions and phase-angle differences[d]
2950 m		2943	CH_2 antisym stretch (101, −162°)
		2940	CH_2 antisym stretch (101, 18°)
2885 s	2890 s	2883	CH_2 sym stretch (100, 175°)
		2873	CH_2 sym stretch (100, −5°)
1470 m		1476	CH_2 scissor (100, 48°)
1453 w	1449 w	1471	CH_2 scissor (100, −132°)
1415 w		1401	CH_2 wag (95, 53°)
1364 m	1364 w	1353	CH_2 wag (107, −129°)
1283 m	1282 s	1286	CH_2 twist (73, −40°)
1236 w	1235 m	1234	CH_2 twist (87, 146°)
1149 s	1143 s	1142	CO stretch (37, −27°), CH_2 rock (29, −66°)
1119 s		1112	CO stretch (81, 136°), CC stretch (21)
1062 m	1064 m	1060	CO stretch (36, −102°), CH_2 rock (35, 70°), CC stretch (17)
947 m		941	CH_2 rock (34, 42°), CC stretch (27), CO stretch (14, 167°)
844 s	846 s	847	CH_2 rock (58, −149°), CO stretch (39, −9°)
	537 w	524	CCO bend (49, −142°), COC bend (21), CH_2 rock (17, 152°)
363 w	363 w	366	CCO bend (42, −73°), COC bend (38)
216 w	216 w	216	CCO bend (48, 64°), CC internal-rotation (28), COC bend (16)
165 w	160 w	164	CC internal-rotation (42), CO internal-rotation (38, −161°), CCO bend (18, 16°)
		92	CO internal-rotation (77, 66°), CCO bend (21, −10°)

a, b, c) See a), b), c) of Table 2.

d) Phase-angle differences $\Delta\varepsilon(OCH_2\text{–}CH_2O)$ are shown for CH_2 sym. and antisym. stretch., scissor., wag., twist., and rock. modes and CCO bend. mode, while $\Delta\varepsilon$(C–O–C) are shown for CO stretch. and internal-rotation modes.

TABLE 4. OBSERVED AND CALCULATED FREQUENCIES (cm^{-1}) AND POTENTIAL-ENERGY DISTRIBUTIONS FOR THE A_1 AND A_2 VIBRATIONS OF PERDEUTERATED POLYETHYLENE GLYCOL $(-CD_2CD_2O-)_p$

	Obs. freq.[a] Infrared[b]	Raman[c]	Calc. freq.	Potential-energy distributions
			2172	CD_2 antisym stretch (102)
			2078	CD_2 sym stretch (101)
			1293	CC stretch (56), CD_2 wag (37)
			1092	CD_2 scissor (57), CO stretch (39)
			1031	CO stretch (47), CD_2 scissor (29)
A_1	inactive		919	CD_2 twist (36), CD_2 rock (21)
			865	CD_2 twist (44), CD_2 wag (24)
			721	CD_2 rock (53), CD_2 twist (20), CO stretch (19)
			245	COC bend (38), CC stretch (21)
			192	CO internal-rotation (34), COC bend (27), CC internal-rotation (21)
	2164 s		2173	CD_2 antisym stretch (102)
	2072 s		2088	CD_2 sym stretch (100)
	1117 vs		1144	CO stretch (84), CD_2 wag (52)
	1087 sh		1080	CD_2 scissor (92)
A_2	996 m	inactive	979	CD_2 twist (35), CD_2 rock (19)
	940 m		950	CD_2 wag (40), CO stretch (21)
	800 m		795	CD_2 twist (46), CCO bend (24), CD_2 rock (23)
	453, 434 w		455	CCO bend (71), CD_2 rock (46)
	95 w		96	CO internal-rotation (88)

a) See a) of Table 2.

b) Ref. 6.

c) Not yet reported.

TABLE 5. OBSERVED AND CALCULATED FREQUENCIES (cm^{-1}), POTENTIAL-ENERGY DISTRIBUTIONS AND PHASE-ANGLE DIFFERENCES FOR THE E_1 VIBRATIONS OF PERDEUTERATED POLYETHYLENE GLYCOL $(-CD_2CD_2O-)_p$

Obs. freq.[a] Infrared[b]	Raman[c]	Calc. freq.	Potential-energy distributions and phase-angle differences[d]
2171 s		2173	CD_2 antisym stretch (103, −97°)
		2172	CD_2 antisym stretch (103, 83°)
2082 s		2089	CD_2 sym stretch (100, 172°)
		2077	CD_2 sym stretch (102, −7°)
1255 m		1252	CC stretch (57), CD_2 wag (41, 15°)
1145 s		1140	CO stretch (72, −158°), CD_2 wag (46, −164°)
1121 s		1116	CO stretch (54, 19°), CD_2 scissor (36, 122°)
1087 sh		1083	CD_2 scissor (76, −83°), CD_2 wag (22, 139°)
1050 w		1040	CD_2 scissor (51, 111°), CO stretch (22, 27°)
1016 s		1001	CD_2 wag (36, −92°), CO stretch (16, 145°), CD_2 twist (12, −45°), CD_2 rock (12, −12°)
942 m		959	CD_2 twist (37, −106°), CO stretch (16, −111°), CD_2 rock (15, −64°)
919 m		905	CD_2 twist (34, 166°), CD_2 rock (31, 86°)
885 w		869	CD_2 twist (61, 42°)
780 w		771	CD_2 rock (30, 46°), CD_2 wag (23, 8°), CD_2 twist (19, 62°)
703 m		699	CD_2 rock (46, −133°), CD_2 twist (33, −135°), CO stretch (21, 3°)
458 w		458	CCO bend (36, −148°), CD_2 rock (26, 155°), COC bend (26)
		320	CCO bend (46, −80°), COC bend (33)
183 w		182	CCO bend (59, 55°), COC bend (14), CO internal-rotation (14, 134°)
156 w		156	CC internal-rotation (62), CO internal-rotation (30, −147°)
		83	CO internal-rotation (78, 64°), CCO bend (20, −4°)

a, b, c) See a), b), c) of Table 4. d) See d of Table 3.

to the effect of nonbonded interaction between methylene-hydrogen atoms and oxygen or carbon atoms. Since the C-O bond length (~1.43 Å) is appreciably shorter than the C-C bond length (~1.54 Å), the repulsive interaction to the methylene-hydrogen atoms of [O-CH_2-C] is expected to be greater than for [C-CH_2-C]. In fact, the repulsion constant of F(HCO)=0.89 mdyn·Å (Table 1) is much larger than F(HCC)=0.32 mdyn/Å. Then, the repulsive interaction is expected to be even greater for polyoxymethylene $[-CH_2-O-]_p$, where a methylene group is bonded to two oxygen atoms. In fact, the wagging constant of polyoxymethylene[24] [f(wa)=0.83 mdyn·Å] is larger than for polyethylene glycol. In accordance with the variation of the wagging constant, the rocking [f(ro)] and twisting constants [f(tw)] increase for the series of polyethylene (0.69 and 0.64 mdyn·Å) or propane (0.73 and 0.66 mydn·Å), polyethylene glycol (0.78 and 0.68 mydn. Å), and polyoxymethylene (1.05 and 0.76 mdyn. Å).

Before comparing the present force field with the force field of earlier normal coordinate treatments, Urey-Bradley force constants of K(CC), K(CO), F(CCO), F(COC), F(HCO) and F(HCC) may be transformed into local-symmetry force constants. Thus, the C-C and C-O stretching constants of polyethylene glycol in earlier treatments[4,6] are derived as f(CC st)=4.72 or 5.11 mdyn/Å and f(CO st)=4.26 or 4.68 mdyn/Å. These values of f(CC st) are much larger than for propane (4.35 mdyn/Å) and polyethylene (4.24 mdyn/Å). On the other hand, the previous values of f(CO st) are much smaller than for dimethyl ether[14] (5.20 mdyn/Å). However, in the present study, the C-C and C-O stretching constants were refined by the method of least squares and now these constants of f(CCst) =4.21 mydn/Å and f(CO st)=5.23 mdyn/Å agree closely enough with the corresponding constants for propane, polyethylene or dimethyl ether. Accordingly, the present set of force constants is considered to be more reasonable than those of earlier treatments. Because of considerable refinements in the force field, vibrational assignments (potential-energy distributions) in the region 1200—800 cm^{-1} were revised as will be presented in the next section.

The internal-rotation constants about the C-C and C-O bonds of polyethylene glycol were refined as f(CC to)=0.113 mdyn·Å and f(CO to)=0.099 mdyn·Å. These values correspond to the internal-rotation potential $V=V_3(1-\cos 3t)/2$ with the barrier height of V_3=3.6 and 3.2 kcal/mol for the C-C and C-O

24) H. Sugeta and T. Miyazawa, Annual Meeting of the Chemical Society of Japan, Tokyo, 1967.

bonds, respectively. These values may be compared with the corresponding values of polyethylene [f(CC to)=0.107 mdy. Å and V_3=3.4 kcal/mol][23] and polyoxymethylene [f(CO to) =0.108 mdyn. Å and V_3=3.5 kcal/mol].[24]

Vibrational Assignments

For the helical chain of polyethylene glycol $[-CH_2-CH_2-O-]_p$, there are seven atoms per repeat unit, so are 10 A_1 and 9 A_2 vibrations, 20 pairs of E_1 and 21 pairs of E_2 vibrations. The A_1, E_1 and E_2 vibrations are Raman active while the A_2 and E_1 vibrations are infrared active giving rise to parallel and perpendicular bands, respectively.

Polarized infrared spectra of polyethylene glycol were measured by Miyazawa *et al.*[4] and Tadokoro *et al.*[5] The Raman effect with mercury-lamp excitation was recorded by Matsui *et al.*[19] Referring to selection rules for infrared and Raman spectra and to observed dichroism of infrared bands, observed frequencies were already assigned[4,6] reasonably to symmetry species of A_1, A_2 or E_1. Recently, Schaufele[20] observed the Raman effect with helium-neon laser excitation (6328 Å) and found a number of Raman lines in the region 3000—25 cm^{-1}. Almost all the A_1, A_2 and E_1 frequencies of the normal species and the A_2 and E_1 frequencies of the perdeuterated species have now been observed as infrared bands and/or Raman lines. These observed frequencies are listed in Tables 2—5, together with frequencies, potential-energy distributions and phase-angle differences calculated in the the present study. Revised vibrational assignments of observed frequencies will be discussed, in contrast to previous assignments.[4,6]

Polyethylene Glycol $(-CH_2CH_2O-)_p$. Infrared bands due to fundamental vibrations of polyethylene glycol in the region 3000—2800 cm^{-1} were identified, with reference to vibrational frequencies of related molecules. Thus, the parallel band at 2890 cm^{-1} and perpendicular band at 2885 cm^{-1} are assigned to the A_2 and E_1 CH_2 symmetric-stretching vibration.[4] The strong Raman line at 2890 cm^{-1} corresponds to the infrared band at 2885 cm^{-1}. The medium-intensity Raman line at 2939 cm^{-1} and the perpendicular infrared band at 2950 cm^{-1} are assigned to the A_1 and E_1 antisymmetric stretching modes, respectively.

The parallel infrared band (doublet at 1463 and 1457 cm^{-1}) and perpendicular bands at 1470 and 1453 cm^{-1} are assigned to the A_2 and E_1 CH_2 scissoring vibrations. The strong Raman line at 1484 cm^{-1} is assigned to the A_1 scissoring vibration while the weak line at 1449 cm^{-1} corresponds to the infrared band at 1453 cm^{-1}.

The Raman line at 1398 cm^{-1} (weak) and parallel infrared band at 1345 cm^{-1} (strong) are assigned to the symmetric (A_1) and antisymmetric (A_2) wagging modes of CH_2-CH_2 groups (Table 2). The two perpendicular bands at 1415 and 1364 cm^{-1} correspond to the CH_2 wagging frequencies of the E_1 species, calculated at 1401 cm^{-1} (with $\Delta\varepsilon=53°$) and at 1353 cm^{-1} (with $\Delta\varepsilon=-129°$), respectively (Table 3). The calculated values of $\Delta\varepsilon$ indicate that the higher-frequency vibration is associated with quasi-symmetric wagging mode of CH_2-CH_2 groups while the lower-frequncy vibration is associated with quasi-antisymmetric mode. The weak band at ~1410 cm^{-1} and strong band at ~1360 cm^{-1} have also been observed for higher oligomers $HO[-CH_2CH_2O-]_pH$ in the crystalline state.[25]

The parallel infrared band at 1244 cm^{-1} is due to the A_2 vibration associated with the antisymmetric twisting mode of CH_2-CH_2 groups. The perpendicular bands at 1283 (medium) and 1236 cm^{-1} (weak) are due to quasi-symmetric ($\Delta\varepsilon=-40°$) and quasi-antisymmetric twisting modes ($\Delta\varepsilon=146°$), respectively, of CH_2-CH_2 groups.*2 It may be remarked that the intensities of the infrared bands at 1244 and 1283 cm^{-1} compare with the intensities of the bands (at 1345 and 1364 cm^{-1}) due to CH_2 wagging modes (see Fig. 2 of Ref. 4). Strong absorption of twisting modes of C-CH_2-O groups has been discussed previously[4] in relation with dissimilarity of C-C and C-O bonds (as for polarity or conformation).

The Raman line observed at 1235 cm^{-1} appears to correspond to the perpendicular infrared band at 1236 cm^{-1} (E_1 species). The Raman line due to the A_1 vibration calculated at 1252 cm^{-1} is possibly overlapped by the Raman line at 1235 cm^{-1}.

Infrared bands and Raman lines in the region 1150—800 cm^{-1} are due to C-C and C-O stretching modes and CH_2 rocking mode. Two parallel infrared bands are assigned to A_2 vibrations (Table 2). The very strong band

25) H. Matsuura and T. Miyazawa, *Spectrochim. Acta*, **23A**, 2433 (1967).

*2 In a previous treatment[4] of potential-energy distributions, CH_2 wagging and twisting modes were considerably mixed for vibrations in the region 1430—1230 cm^{-1}. However, with the force field refined in the present study, vibrations calculated above 1340 cm^{-1} are almost purely associated with CH_2 wagging modes and vibrations below 1290 cm^{-1} are associated with twisting modes.

at 1102 cm^{-1} is associated almost exclusively with the C-O-C antisymmetric stretching mode while the strong band at 963 cm^{-1} is associated primarily with the antisymmetric rocking mode of CH_2-CH_2 groups.

The medium-intensity Raman lines at 1126 and 861 cm^{-1} are assigned to the A_1 vibrations calculated at 1137 and 866 cm^{-1}, respectively (Table 2). As for potential-energy distributions, these lines are due to hybridized vibrations of the CH_2-CH_2 symmetric rocking mode and C-O-C symmetric stretching mode. For the A_1 species, the C-C stretching mode is coupled with the C-O-C symmetric stretching mode, to yield the vibration calculated at 1073 cm^{-1}. However, a corresponding Raman line has not been identified, possibly because of overlap with the medium-intensity line at 1064 cm^{-1}.

The Raman line at 1143 (strong), 1064 (medium) and 846 cm^{-1} (strong) correspond to the perpendicular infrared bands (E_1 species) at 1149 (strong), 1062 (medium) and 844 cm^{-1} (strong). The vibration calculated at 1142 cm^{-1} is associated with quasi-symmetric C-O stretching mode and CH_2 rocking mode,*3 whereas the vibration calculated at 847 cm^{-1} is associated with quasi-antisymmetric ($\Delta\varepsilon=-149°$) CH_2 rocking mode and quasi-symmetric ($\Delta\varepsilon=-9°$) C-O stretching mode. The vibration calculated at 1060 cm^{-1} is also associated with the C-O stretching ($\Delta\varepsilon=-102°$) and CH_2 rocking mode ($\Delta\varepsilon=70°$).

The strong perpendicular band at 1119 cm^{-1} is primarily due to quasi-antisymmetric ($\Delta\varepsilon=136°$) C-O stretching mode as coupled with the C-C stretching mode. The medium-intensity band at 947 cm^{-1} is due largely to CH_2 quasi-symmetric ($\Delta\varepsilon=42°$) rocking mode and C-C stretching mode. This perpendicular band at 947 cm^{-1} together with the bands at 963 and 844 cm^{-1} have been discussed[26-29] in relation with the conformation of O-CH_2-CH_2-O groups. However, vibrational assignments of these bands are now established after the refined treatment of the present study.

A weak Raman line has been observed at 930 cm^{-1} by Matsui *et al.*[19] or at 936 cm^{-1} by Schaufele.[20] This line does not correspond to any calculated A_1 frequencies or to perpendicular infrared bands (E_1) in this region. As mentioned previously, E_2 vibrations are infrared inactive but they are active in the Raman effect. Accordingly, the Raman line at 936 cm^{-1} may be assigned to the E_2 vibration (with the phase difference of $\delta=2\theta$) calculated at 922 cm^{-1}. This E_2 vibration is associated with the C-C stretching and C-O stretching modes.

Chain vibrations of polyethylene glycol in the region below 600 cm^{-1} are associated with C-C-O and C-O-C bending modes and internal-rotation modes about C-C and C-O bonds. Raman lines have been observed at 537, 363, 279, 216 and 160 cm^{-1}, parallel infrared bands at 529, 508 and 107 cm^{-1}, and perpendicular bands at 216 and 165 cm^{-1}. In the present study, a weak band was found at 363 cm^{-1} for Carbowax 6000 (high molecular-weight polyethylene glycol from Carbide and Carbon Chemicals Corporation).

The parallel band (doublet at 529 and 508 cm^{-1}) corresponds to the A_2 vibration calculated at 533 cm^{-1}. This is the C-C-O bending vibration as coupled with the CH_2 rocking mode. The doublet splitting is either due to Fermi resonance with combination vibrations or to interchain ineractions in the crystalline lattice.[4] In the present study, therefore, the infrared absorption (600—400 cm^{-1}) was measured for solid solutions of Carbowax 6000 and *n*-octacosane ($C_{28}H_{58}$)*4 with the mixing weight-ratio of 1 : ~50. At this low concentration, any interchain effect is reduced negligible. However, the peak positions and relative intensities of the doublet in the solution are still the same as in the crystalline state. This observation indicates that the doublet splitting is possibly due to Fermi resonance rather than to interchain interactions. Therefore, the dispersion curves (frequency *versus* phase difference) of the polyethylene-glycol chain[30] were reviewed, for possibilities of Fermi resonance with the A_2 fundamental calculated at 533 cm^{-1}. In fact, the splitting may now be ascribed to the Fermi resonance between the A_2 fundamental

*3 In previous treatments[4,6] the potential energy for the A_1 vibration at 1126 cm^{-1} and the E_1 vibration at 1149 cm^{-1} was largely associated with the C-C stretching mode, because the C-C stretching constant was perphaps too large and the C-O stretching constant was too small.

*4 In the region 600—400 cm^{-1}, *n*-octacosane exhibits only aweak peak at 564 cm^{-1}.

26) W. H. T. Davison, *J. Chem. Soc.*, **1955**, 3270.
27) Y. Kuroda and M. Kubo, *J. Polymer Sci.*, **26**, 323 (1957); **36**, 453 (1959).
28) H. F. White and C. M. Lovell, *J. Polymer Sci.*, **41**, 369 (1959).
29) A. Miyake, *J. Am. Chem. Soc.*, **82**, 3040 (1960).
30) H. Sugeta, H. Matsuura and T. Miyazawa, International Symposium on Macromolecular Chemistry, Tokyo, 1966.

*5 Another resonance may also be expected between the A_2 fundamental and the binary combination of B_1 (calc. 196 cm^{-1}) and B_2 (calc. 289 cm^{-1}) vibrations. The symmetry species for overtones and combinations have been given.[12,31]

and the binary combination of the E_1 vibrations [363+165=528 cm^{-1}].*5

The Raman lines at 537 cm^{-1} (E_1) and 279 cm^{-1} (A_1), Raman line and infrared band (perpendicular) at 363 cm^{-1} (E_1) are assigned to the hybridized vibrations of C-O-C and C-C-O bending modes. The perpendicular band at 216 cm^{-1} is assigned to the E_1 vibration associated with the quasi-symmetric C-C-O bending mode and C-C internal-rotation mode. The weak Raman line at 216 cm^{-1} corresponds to this E_1 vibration and/or to the A_1 vibration (calculated at 218 cm^{-1}) which is associated with the C-O-C bending mode and symmetric internal-rotation mode about C-O bonds.

The perpendicular infrared band at 165 cm^{-1} (and corresponding Raman line at 160 cm^{-1}) is due to the hybridized vibration of the C-C internal-rotation mode and quasi-antisymmetric internal-rotation mode about C-O bonds. The parallel band at 107 cm^{-1} is due to the antisymmetric internal-rotation mode about C-O bonds.

A weak infrared band[2] is observed at 580 cm^{-1} and the corresponding Raman line[20] at 584 cm^{-1}. Accordingly, this vibration is assigned to the E_1 species. There is no E_1 fundamental calculated around this frequency. However, the observed vibration may be assigned reasonably to the combination (E_1 species) of the A_1 vibration at 216 cm^{-1} and the E_1 vibration at 363 cm^{-1}. Supporting this assignment, the corresponding band (shoulder) is observed[6] around 500 cm^{-1} for the perdeuterated species, just as expected for the combination of the A_1 and E_1 vibrations calculated at 192 and 320 cm^{-1}, respectively.

The Raman lines at 126 and 75 cm^{-1} can not be explained as due to chain vibrations of A_1, E_1 or E_2 species, and are possibly due largely to lattice modes. Intensities or positions of the bands due to lattice vibrations are sensitive to temperature changes. In fact, Schaufele[32] observed that, at lower temperature, the Raman lineat 126 cm^{-1} intensifies relative to the line at 75 cm^{-1}.

Polyethylene-d_4 Glycol $(-CD_2CD_2O-)_p$. The strong parallel band of polyethylene-d_4 glycol at 1117 cm^{-1} is due to the A_2 vibration associated with the antisymmetric C-O stretching and CD_2 wagging modes (Table 4). Similarly the strong perpendicular band at 1145 cm^{-1} is due to the E_1 vibration associated with quasi-antisymmetric C-O stretching ($\Delta\varepsilon=-158°$) and CD_2 wagging modes ($\Delta\varepsilon=164°$). On the other hand, the E_1 vibration at 1121 cm^{-1} is due to quasi-symmetric C-O stretching mode ($\Delta\varepsilon=19°$) as coupled with quasi-antisymmetric CD_2 scissoring mode ($\Delta\varepsilon=122°$) (Table 5). The infrared bands, at 1050 and 1087 cm^{-1}, primarily due to CD_2 scissoring modes are weak and not well-defined. The C-C streching mode is strongly coupled with quasi-symmetric CD_2 wagging mode, giving rise to the medium-intensity infrared band at 1255 cm^{-1} (E_1). Infrared bands in the region 1000—700 cm^{-1} are due to hybridized vibrations of CD_2 wagging, twisting and rocking modes and C-O stretching mode.

In the region below 500 cm^{-1}, infrared bands due to skeletal bending and internal-rotation modes are observed. Similar to the doublet bands (529 and 508 cm^{-1}) of the normal species, doublet bands with parallel dichroism are again observed at 453 and 434 cm^{-1} for the perdeuterated species. This doublet, in fact, corresponds to the A_2 vibration calculated at 455 cm^{-1}, which is associated with the CCO bending mode heavily coupled with the CD_2 rocking mode. The doublet splitting is reasonably ascribed to the Fermi resonance between the A_2 fundamental and the combination of E_1 vibrations [320+156=476].*6 The perpendicular bands at 458 and 183 cm^{-1} are largely due to quasi-antisymmetric and quasi-symmetric bending modes, respectively, of O-C-C-O groups. The infrared bands of the deuterated species at 95 cm^{-1} (parallel) and 156 cm^{-1} (perpendicular) correspond to the bands of the normal species at 107 and 165 cm^{-1}, respectively, and are assigned to internal-rotation modes about C-O and C-C bonds.

31) G. Herzberg, "Molecular Spectra and Molecular Structure," Vol. II, D. Van Nostrand Co., Inc., New York (1945), p. 123.

32) R. F. Schaufele, private communication.

*6 Another possibility is the resonance with the combination of the B_1 and B_2 vibrations calculated at 175 and 247 cm^{-1}, respectively.